COUPLED THERMAL-MAGNETIC ANALYSIS OF A SATURATED PERMANENT MAGNET MOTOR

Johan Driesen, Herbert De Gersem, Ronnie Belmans and Kay Hameyer

KATHOLIEKE UNIVERSITEIT LEUVEN, DEP. EE (ESAT), DIV. ELEN
Kardinaal Mercierlaan 94, B-3001 Heverlee, Belgium
johan.driesen@esat.kuleuven.ac.be http://www.esat.kuleuven.ac.be/elen/elen.html

Abstract
In order to obtain an accurate simulation of a saturated permanent magnet machine designed for servo applications, both magnetic and thermal fields have to be calculated in a coupled simulation. The temperature dependency of the magnetic and electric material characteristics of the conductors and the permanent magnetic materials has to be considered. The combination of several algorithms are leading to the overall solution of the fields. This approach is illustrated by a coupled simulation of a small permanent magnet motor for automotive applications. For this example, the performance characteristics versus the operating range of environment temperatures are calculated.

1. - INTRODUCTION

To predict the performance of electromechanical devices, already in the design stage, a coupled simulation is recommended due to the strong dependency of the material characteristics on temperature. This leads to a non-linear system of partial differential and algebraic equations which can be solved by applying finite element methods and adaptive relaxation techniques.
Using this approach, a better prediction of the change of the torque-speed characteristics at extreme environmental temperatures is made and eventually the demagnetisation point is predicted more accurately. This knowledge can be used to optimise the design of machines within an electrical drive system operating in changing environmental circumstances. As an illustration of the coupled calculations, the simulations of a small saturated permanent magnet servo motor are used.

3. - MAGNETIC-THERMAL COUPLED CALCULATIONS OF PM-MACHINES

2.1 - Magnetic sub-problem

The material properties of permanent magnets are temperature sensitive. Therefore, the flux in permanent magnets depends on the temperature. The point of irreversible demagnetisation of the magnets is reached much earlier. All magnetic materials lose their properties beyond a certain transition temperature, the Curie temperature.
The behaviour of permanent magnet machines is described by differential equation (1).

$$\begin{aligned}&\nabla\left(\nu\left(\boldsymbol{A},\boldsymbol{T}\right)\cdot\nabla\boldsymbol{A}\right)-\sigma(\boldsymbol{T})\cdot(\boldsymbol{v}\bullet\nabla\boldsymbol{A}-\nabla\boldsymbol{V})\\&=-\nabla\left(\upsilon_0\nu_{\boldsymbol{rev}}(\boldsymbol{T})\cdot\boldsymbol{M}(\boldsymbol{T})\right)\end{aligned}\qquad(1)$$

with *A* the magnetic vectorpotential ($\nabla\times\boldsymbol{A}=\boldsymbol{B}$) and $\boldsymbol{V}$ the voltage drop along the conductors. $\boldsymbol{v}$ represents the local speed vector [1]. The saturation and the coupling to the temperature through the electrical conductivity σ and the permanent magnet data υ and *M* make this a non-linear problem formulation.
The second term on the left-hand side represents the current density $\boldsymbol{J}=-\sigma\cdot\nabla\boldsymbol{V}$. If the current source density is known, it moves to the right-hand side. Otherwise it resides, and extra (circuit) equations [2] have to be added to compute *V*. This introduces numerical difficulties due to the different algebraic

nature of these equations. External lumped parameter models for brushes, for example, can be included in this part.
Often, the motional term between the brackets, describing the induced voltage due to motion, can be omitted without affecting the precision of the solution when no skin effects can occur (e.g. stranded conductors), but remains in the circuit part.

2.2 - **Thermal subproblem**

$$\nabla\left(\boldsymbol{k}(\boldsymbol{T})\cdot\nabla\boldsymbol{T}\right) = -\boldsymbol{p}_{\Omega} - \boldsymbol{p}_{\boldsymbol{Fe}}$$
$$\boldsymbol{p}_{\Omega} = \frac{\boldsymbol{J}^2}{\sigma(\boldsymbol{T})} \qquad (2)$$
$$\boldsymbol{p}_{\boldsymbol{Fe}} = \boldsymbol{f}(\omega, \boldsymbol{B})$$

Ohmic losses in the armature winding are assumed to be the heat sources. They are calculated based on the currents *J* withdrawn from the magnetic solution.
Ferromagnetic losses p_{FE} are generated in the rotor for a dc-type PM-machine respectively in the stator of a brushless dc-machine and are a function of the magnetic field *B* and rotation speed. Eddy currents may occur in conducting magnets [3].
Most of the heat source terms are expressed by non-linear functions of the solution of the magnetic problem. The thermal conductivity *k* is a function of the temperature itself.

2.3 - **Discretisation by means of the FEM**

The equations are discretised by applying a Galerkin approach on a triangular FEM-mesh. This leads to a non-symmetric system of equations for the magnetic part due to the directional character of the term describing the motional induced voltage. If necessary, these equations are completed by a set of electric circuit equations containing temperature dependent parameters as well such as the resistivity of the conductor material.
The thermal equation leads to a symmetric system of equations.
These different types of large-scale systems are solved very efficiently individually with an appropriate, pre-conditioned iterative solver. In case of the non-symmetric equations this would be SORBiCG whereas the symmetrical equations are better solved by a SSORCG algorithm.

2.4 - **Coupled problem solution strategies**

The coupling of the magnetic and the thermal field can be accomplished in two different ways:

- Full or numerical strong coupling
- Cascade or numerical weak coupling

A very obvious way is to directly treat the coupled system by solving the complete set of fully coupled non-linear equations. After discretisation, this may lead to an extensive system of algebraic equations describing phenomena with different time constants [4]. To linearise this coupled system of equations a database containing sufficient information to determine the interdependencies of the material characteristics on the solution variables has to be present [5]. If a Newton algorithm is applied in a non-linear iteration, the partial derivatives have to be known. This system of equations results in the total solution vector, but is hard to solve in practice due to different numerical properties of the underlying subproblems.
An alternative strategy consists of the decomposition of the multi-field problem into a cascade of (non-linear) sub-problems, each covering a single physical field. The sub-problems are solved sequentially by well-suited numerical algorithms in an iteration loop until convergence is obtained. Intermediately, the coupling terms such as the heat sources are calculated and the material parameters are adjusted per mesh element based on the solutions of the previous steps [6] [7]. To obtain a fast convergence, an adaptive relaxation algorithm is required. In general, this approach is very flexible. The algorithm can be adapted easily for different types of motors with different loss mechanisms and materials.

3. - **APPLICATION**

3.1 - **Motor designs**

This approach is illustrated on a small 14V-50W permanent magnet brushed dc motor for automotive applications with a full load speed of 100 rev/s [8] in an intermitted duty. Its range of operation is required from -40°C to +180°C. The armature is wound in two layers. The permanent magnet demagnetisation characteristic is influenced by the temperature which leads to deviate operations under the extreme temperatures.
The design is made for two types of permanent magnet materials, a typical ferrite and a NdFeB alloy. Due to the different magnet characteristics, the rare-earth magnet design leads to a thinner magnet and hence a smaller motor. These materials have different temperature dependencies. In general rare-earth materials have larger temperature coefficients and therefore, the decline of the flux at higher temperatures increases. The major data necessary for the calculations

is found in table 1, which is based on some typical commercially available materials.
The necessary purely magnetic data are the remanent field B_r and the relative permeability μ_r. The temperature dependency is expressed by two thermal coefficients, valid for the linear part of the magnetisation characteristic in which all regular operation points must be found (Fig.1):

- α_{Br} describes the linear temperature shift of the remanent field

$$\boldsymbol{B_r}(\boldsymbol{T}) = \boldsymbol{B_{r,T_{ref}}}\left(1+\alpha_{\boldsymbol{B_r,T_{ref}}}\left(\boldsymbol{T}-\boldsymbol{T_{ref}}\right)\right) \qquad (3)$$

- $\alpha_{Hc'}$ models the linearised change of the coercitivity H_c^* and H_c^* stands for the linearly extrapolated value of the coercitive field.

$$\boldsymbol{H_c}(\boldsymbol{T}) = \boldsymbol{H_{c,T_{ref}}}\left(1+\alpha_{\boldsymbol{H_c,T_{ref}}}\left(\boldsymbol{T}-\boldsymbol{T_{ref}}\right)\right) \qquad (4)$$

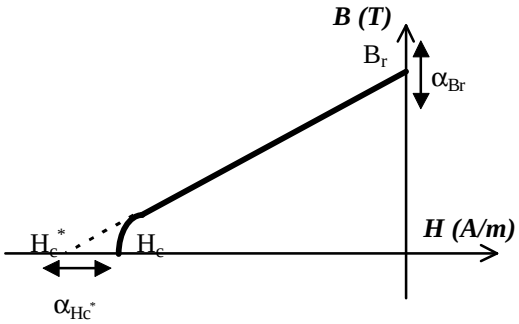

Fig. 1: Demagnetisation characteristic of permanent magnet material.

Material	B_r *[T]*	μ_r	*thickness [mm]*
Ferrite	0.28	1.1	8
NdFeB	0.52	1.25	1.4

Table 1a: major magnetic and design characteristics of the permanent magnets.

Material	α_{Br}	$\alpha_{Hc'}$	*k [W/mK]*
Ferrite	-0.002	-0.002	2
NdFeB	-0.001	-0.005	10

Table 1b: major thermally related characteristics of the permanent magnets.

3.2 - **Thermal modelling of the air gap**

The largest part of the heat flows from the rotor through the air gap to the stator, where it is transmitted to the surrounding air by natural convection [9]. Hence, a major part of heat flows through the permanent magnet. The rest of the heat is transport by conduction through the shaft or is taken away by a forced axial cooling flow if forced ventilation is foreseen.
An important part of the thermal model is therefore the representation of the air gap. In the finite element model, the air is defined by an equivalent conductivity, of which the value is calculated based on fluid-dynamics considerations.
In a first step, the flow regime in the air gap is determined. The calculation of the Taylor number of the flow demonstrate that no vortices arise and that the transport will be laminar [10]. Hence the main heat transport mechanism in the air gap is conductive.
From experiments described in literature [11], a Nusselt number can be estimated for this flow. This has to be augmented by 30% because of the non-smooth surfaces causing recirculating flows. The non-smoothness of the rotor has the largest effect influence on this.
This leads to an estimate for the surface heat transfer coefficients for the rotor and stator surface. For these types of flows, the temperature dependency of the parameters can be neglected.
In the classical lumped parameter thermal models a series connection of two thermal resistances is calculated based on these values [12]. To derive an equivalent thermal conductivity $k_{eq,air}$, this is assumed to be equal to a thermal resistance of an cylindrical component with the dimensions of the air gap.

$$\frac{1}{h_{stat}\,A_{stat}}+\frac{1}{h_{rot}\,A_{rot}}=\frac{ln\left(\left(r_{stat}-h_{magnet}\right)\Big/ r_{rot}\right)}{2\pi\cdot k_{eq,air}} \qquad (5)$$

3.4 - **Coupling of the magnetic and thermal models**

The coupling of both models is not straightforward if the stationary thermal field is the objective of the calculation. The magnetic subproblem leads to a static solution of the magnetic field. If this would be used to calculate the joule losses in the armature winding, a temporary figure of those losses would be the result. This means that the conductors involved in the commutation process would not generate heat. On the other hand, the input of the thermal model must be an average loss in order to obtain a static thermal image. Therefore, some intermediate calculations must be performed:

- Time-averaging of the temporary heat losses over the conductors. This can be done approximately, by averaging over the slots as modelled in the static solution (spatial averaging).
- Multiplication with the duty factor to account for the intermitted operation.

3.3 - **Dual thermal model of the air gap**

From the thermal model, the temperature of the stator magnet region and the rotor conducting regions has to be retrieved to serve as an input for the magnetic model. For machines with an almost smooth air gap (e.g. induction machines), it is possible to retrieve that information from only one model. Here, however, the air gap is not smooth due to the surface-mounted magnet shells and hence the path of the heat flow is not fully axisymmetric.

From the viewpoint of the stator (static frame), the fast revolving rotor can be modelled as a rotating cylinder with the averaged heat sources, estimated in the magnetic problem. The first model, referred to the stator, contains the air gap and the magnet shells in their correct geometry (Fig. 2a). The resulting thermal field in the stator will be used to update the temperature depending magnetic properties of the permanent magnet.

A second model is referred to the rotor (Fig. 2b). The heat sources are averaged to obtain the static field. The heat path through the air gap is changing periodically as seen from the revolving rotor. Therefore, to obtain a constant heat flow density from the rotor surface, an equivalent axisymmetric material must be assumed, filling the air and the magnet regions and representing the average flow path. The equivalent thermal conductivity k_{avg} of this material can be calculated by equation (6).

$$\frac{\pi}{\beta_p}\cdot\left[\frac{ln\left(\left(r_{stat}-h_{magn}\right)/r_{rot}\right)}{2\pi\cdot k_{eq,air}}+\frac{ln\left(r_{stat}/\left(r_{rot}+h_{airgap}\right)\right)}{2\pi\cdot k_{magnet}}\right] \quad (6)$$
$$+\frac{\pi}{\pi-\beta_p}\cdot\frac{ln\left(r_{stat}/r_{rot}\right)}{2\pi\cdot k_{eq,air}}=\frac{ln\left(r_{stat}/r_{rot}\right)}{2\pi\cdot k_{avg}}$$

For the stranded conductors, an average thermal conductivity can be deduced, accounting for the isolation and the size of the strands. An extra thermal contact resistance between them can be modelled as well.

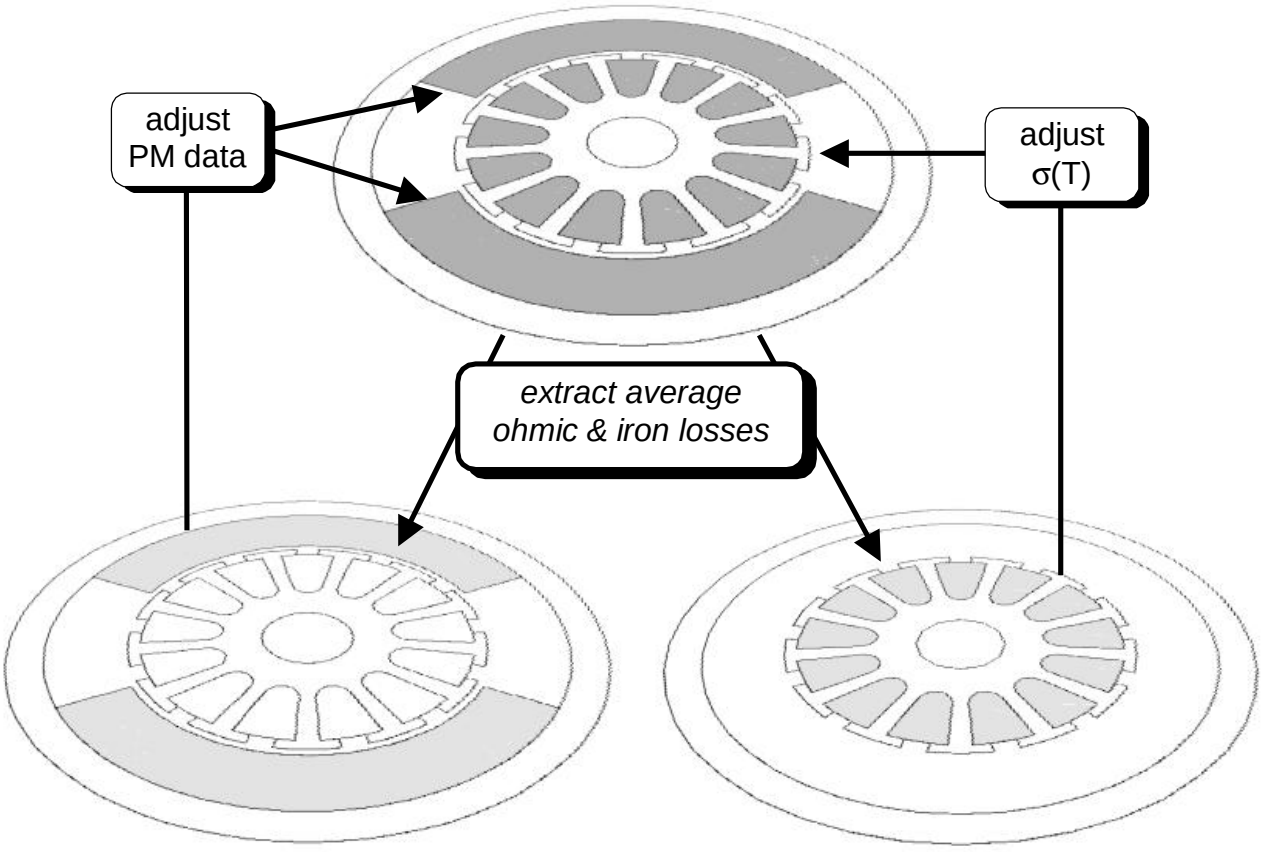

Fig. 2 : Relation between magnetic and thermal models.

4. - **RESULTS**

The computations are performed on a mesh containing 8892 triangular element of first order for the ferrite design. Because of the smaller geometry of the NdFeB model, only 7748 elements are used (Fig. 3).

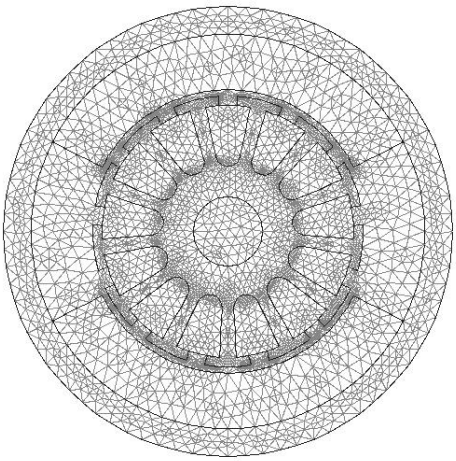

Fig. 3: Discretisation for the ferrite design.

After the coupled field problem converges, an accurate solution of both, the magnetic and thermal field (Fig. 4, 5) is obtained. It is used to calculate the torque and other motor performance characteristics such as the efficiency.

Because of the differences in thickness between the alternative designs and the difference in thermal conductivity (table 1), a larger temperature difference between stator and rotor can be noticed for the ferrite design.

Table 2 contains temperatures and heat loss densities resulting out of the calculation at selected environmental temperatures.

Surrounding air temp. [°C]	q_{Cu} *[W/m³]*	T_{Cu} *[°C]*	T_M *[°C]*
-40	$9{,}38.10^4$	-21,3	-26,9
25	$1{,}29.10^5$	50,8	43,0
100	$1{,}70.10^5$	134,0	123,4
180	$2.13.10^5$	222,6	209,4

Table 2a: Thermal solution data at selected environmental temperatures (ferrite design).

Surrounding air temp. [°C]	q_{Cu} *[W/m³]*	T_{Cu} *[°C]*	T_M *[°C]*
-40	9,43.104	-20,1	-24,8
25	$1{,}29.10^5$	52,4	46,0
100	$1{,}71.10^5$	136,1	127,6
180	$2.15.10^5$	225,3	214,7

Table 2b: Thermal solution data at selected environmental temperatures (NdFeB design).

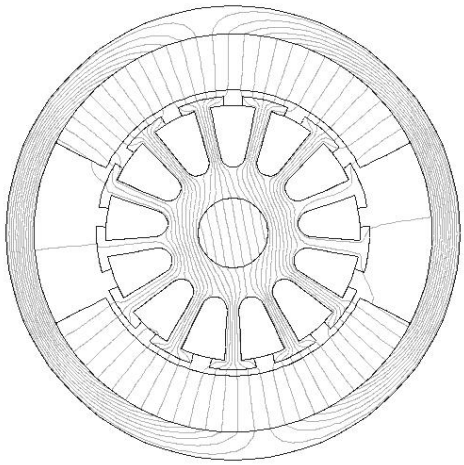

Fig. 4: Plot of the magnetic flux lines (ferrite design).

It must be noted that during the iteration process, the operation point on the permanent magnet characteristic can oscillate heavily. This happens when an inappropriate or no relaxation is applied to the adjustment of the material data within the non-linear iteration loop. In that case, a non-smooth convergence towards the solution of the non-linear coupled problem or, in some cases, a divergence may be obtained.

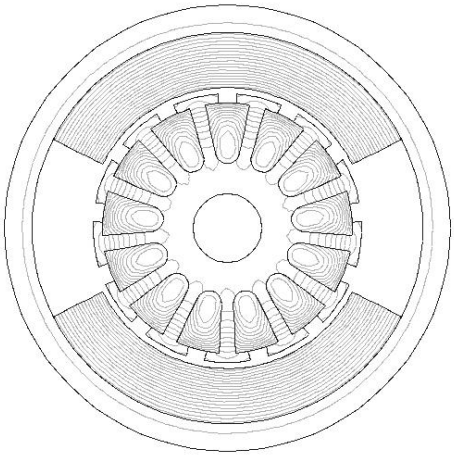

Fig. 5: Composite plot of the isothermal lines (ferrite design); fields lines in the air gap are not shown since an equivalent, none physical material was assumed there.

Figure 6 shows the torque characteristics relative to the nominal torque at a standard temperature of 25°C for the different designs in rated conditions. In this case, a constant armature current is assumed.

This figure shows the higher temperature sensitivity of the NdFeB design. The torque drops almost linearly when the temperature increases. At lower temperatures, the torque rises as the permanent magnet flux becomes higher, causing the machine to saturate stronger. This leads to a non-linear characteristic at low temperatures. This is also noticed in the convergence rate of the algorithm: due to the higher saturation level, more non-

linear steps are necessary during the solving of the systems of equations.

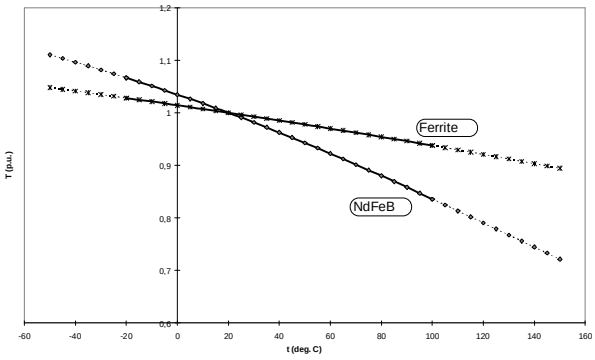

Fig. 6: Torque characteristic (rated conditions) for an increasing temperature of the surrounding air (the full lines cover the rated operating range).

Related characteristics such as torque characteristics at rated constant voltage or speed characteristics can be derived as well. In that case the circuit equations, holding temperature dependent resistances, have a larger impact.

5. - **CONCLUSION**

A coupled design approach is necessary for permanent magnet machines operating over a large temperature range. Especially the temperature dependency of the permanent magnet material characteristics leads to an important change in performance characteristics. These effects can be considered by applying a relaxed coupled FEM-simulation. This is illustrated for a saturated dc permanent magnet machine. The approach can be generalised towards other types of electrical machines containinf permanent magnets such as brushless dc-machines with non-smooth air gaps.

ACKNOWLEDGEMENT

The authors are grateful to the Belgian “Fonds voor Wetenschappelijk Onderzoek Vlaanderen” for its financial support of this work and the Belgian Ministry of Scientific Research for granting the IUAP No. P4/20 on Coupled Problems in Electromagnetic Systems. The research Council of the K.U.Leuven supports the basic numerical research. J. Driesen holds a research assistantship of the Belgian “Fonds voor Wetenschappelijk Onderzoek - Vlaanderen”.

REFERENCES

[1] Binns, K.J.; Lawrenson, P.J.; Trowbridge, C.W.: *The Analytical and Numerical Solution of Electric and Magnetic Fields.* John Wiley & Sons, Chichester, Reprint 1994.

[2] De Gersem, H.; Mertens, R.; Pahner U.; Hameyer, K.; Belmans, R.: *Coupled field-circuit problem: a generalized signal flow graph description of the circuit equations*. 2nd Conf. Eur. sur les Méthodes Numériques et Electromagnétiques, Lyon, France, 19-21 March ’97, pp. CP1-07.

[3] Polinder, H.; Hoeijmakers, M.J:. *Eddy-current losses in the permanent magnets of a PM machine*. IEE Conf. on Electrical Machines & Drives, Cambridge, UK, September 1-3, 1997, pp. 138-142.

[4] Molfino, P.; Repetto, M.*: Comparison of Different Strategies for the Analysis of Non-linear Coupled Thermo-Magnetic Problems under Pulsed Conditions*. IEEE Trans. on Magnetics, vol. 26, no. 2, pp. 559-562.

[5] Driesen, J.; Fransen, J.; De Gersem, H.; Hameyer, K.; Belmans, R.: *Object oriented storage of material data for coupled problems*. XIth conference on the computation of electromagnetic fields (COMPUMAG), Rio de Janeiro, Brazil, Nov. 2-6, 1997, paper PB4-7, pp.195-196.

[6] Hameyer, K.; Pahner, U.; Belmans, R.; Hedia, H.: *Thermal computation of electrical machines*. 3rd international workshop on electric & magnetic fields”, Liège, Belgium, May 6-9, 1996, pp.61-66.

[7] Chaboudez, C.; Clain, S.; Glardon, R.; Mari, D.; Rappaz, J.; Swierkosz, M.: *Numerical Modeling in Induction Heating for Axisymmetric Geometries*. IEEE Trans. on Magnetics, vol. 33, no. 1, pp. 739-745.

[8] Hamdi, E.S.: *Design of small electrical machines.* Wiley (1994).

[9] Liu, Z.; Howe, D.; Mellor, P.; Jenkins, M.: *Thermal analysis of permanent magnet machines.* 6th Int. Conf. On Electrical Machines & Drives, 1993, pp. 359-364.

[10] Saari, J.: *Friction losses and heat transfer in high-speed electrical machines.* Helsinki University of Technology, Laboratory of Electromechanics, report no. 50, Espoo, Finland.

[11] Gazley, C.: *Heat-transfer characteristics of the rotational and axial flow between concentric cylinders.* Trans. of the ASME, vol. 80, jan. 1958, pp. 79-90.

[12] Mellor, P.H.; Roberts, D.; Turner, D.R.: *Lumped parameter thermal model for electrical machines of TEFC design*. IEE Proceedings-B, vol. 138, no. 5, april , pp. 205-218.